Dependence of critical current on voltage probe spacing in superconducting tape with multiple small cracks and a large crack

Ochiai, Shojiro; Okuda, Hiroshi; Fujii, Noriyuki

Materials Transactions, Vol. 60, No. 4 (2019) pp. 574 to 582

Dependence of Critical Current on Voltage Probe Spacing in Superconducting Tape with Multiple Small Cracks and a Large Crack

Shojiro Ochiai[1], Hiroshi Okuda[2] and Noriyuki Fujii[2,*]

[1]*Elements Strategy Initiative for Structural Materials, Kyoto University, Kyoto 606-8501, Japan*
[2]*Department of Materials Science and Engineering, Kyoto University, Kyoto 606-8501, Japan*

In four probe sensing for measurement of voltage-current curve of superconducting layer-coated tapes, it has been reported that, when a large accidental defect is included in the region between the voltage probes, the critical current value estimated with the one micro-volt/cm criterion is low when the voltage probe spacing is small but it becomes higher when the spacing is larger. In the present work, a simulation study was carried out to reproduce the feature stated above and to describe the dependence of critical current value on the voltage probe spacing under the co-existence of a large crack and multiple small cracks. In simulation, the current shunting model at cracks and a Monte Carlo simulation method were applied to a model superconducting tape, which was composed of one local section with a large crack and multiple local sections with small cracks of different size from each other. The experimentally observed increase in critical current with increasing voltage probe spacing in the large defect included tape was reproduced well by the present simulation. Then, it was shown that the increase in critical current of the large crack-included region with increasing voltage probe spacing is caused by the increase in the ligament part-transported current and shunting current at the large crack due to the increase in critical voltage for determination of critical current. Furthermore, it was shown that the upper and lower bounds of the critical current of the region, in which a large crack and multiple small cracks exist, can be derived from the voltage-current curve of the section with a large crack, and the critical current of the region is given by the upper bound for a given size of the largest crack when the difference in size between the large crack and multiple small cracks is large. [doi:10.2320/matertrans.MBW201803]

(Received October 16, 2018; Accepted December 5, 2018; Published January 21, 2019)

Keywords: *coated conductor, heterogeneous cracking, critical current, voltage probe spacing, modeling analysis*

1. Introduction

Thermal, mechanical and electromagnetic stresses are exerted to superconducting layer-coated tapes as well as superconducting filaments-embedded tapes in fabrication and in operation. When the superconducting layers/filaments are cracked under high stresses, the critical current (I_c)–values of coated[1–12] and filamentary[13–22] conductor tapes are seriously reduced. The extent of cracking is different from location to location within a tape. Accordingly, properties such as critical current and n-value of the tape depend on the position-dependent crack size, and they are dependent on the specimen length.[9,22]

In measurement of voltage (V)–current (I) curves, the four probe–sensing method is popularly used. Concerning the influence of voltage probe spacing on the variation of critical current along the length, it has been reported that local information of critical current values in a specimen is diluted when the voltage probe spacing is large.[23] Also, under existence of heterogeneous defects/cracks, the following feature has been observed experimentally.[9,22,23]

Figure 1 shows a schematic representation of the influences of the voltage probe spacing on variation of critical current with position in tape under existence of a large crack at the central position $x = 0$ and multiple small cracks of different size at the positions other than the central position, where the large crack is an extra-ordinary one which may be introduced accidentally or may appear as an extreme case under statistical distribution. When the voltage probe spacing is small as in (a), the critical current value of the region between the voltage probes, containing a large crack and multiple small cracks, is low. However, when the probe spacing is large as in (b), the critical current value of the region, containing the same large crack and more number of small cracks, is high in comparison with that in (a). Such a probe spacing-dependence of critical current value is dangerous in practical use.[23] The importance of study on statistical inhomogeneity and accidental one along the longitudinal direction has been designated for practical system design.[24]

The aim of the present work is to reproduce the feature shown in Fig. 1 by using a simulation method developed recently by the authors,[10–12] which is based on a Monte Carlo simulation method combined with a model of crack-induced current shunting.[13] We have been applying this simulation method to investigate the influences of the statistical crack size distribution and voltage probe spacing on critical current- and n-values. With this simulation method, the experimentally observed features that the critical current- and n-values decrease with increasing width of crack size distribution and voltage probe spacing/specimen length, and the width of critical current distribution decreases with increasing voltage probe spacing[9–22] has been reproduced successfully.[10–12]

In the present work, the case where one accidental large crack exists in addition to the multiple small cracks, whose size distribution is statistically describable, was taken up, and the influence of voltage probe spacing on the variation of critical current along the tape length in RE(Y, Sm, Dy, Gd, …)$Ba_2Cu_3O_{7-\delta}$ layer-coated tapes (hereafter noted as REBCO tapes) was studied by arranging the simulation method for the present purpose.

2. Model for Analysis

2.1 Model tape

Figure 2 shows a schematic representation of the model tape consisting of sections with a length $L_0 = 1.5$ cm,

*Graduate Student, Kyoto University

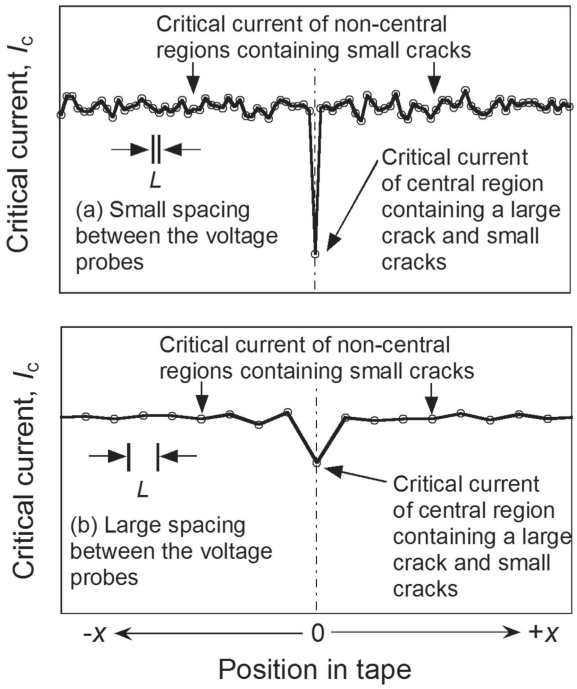

Fig. 1 Schematic representation of the influence of the voltage probe spacing L on the variation of critical current value with position along the tape length direction under co-existence of a large crack and multiple small cracks. (a) and (b) refer to the cases of small and large spacing between the voltage probes, respectively.

together with the x coordinate. The tape consists of 205 sections. Each section has a crack with different size from each other. The section existing at the center part of the specimen is called as a central section. The other sections are called as non-central sections. The position of the crack in the central section is set to be $x = 0$. The other cracks exist at $x = \pm L_0$, $\pm 2L_0$, $\pm 3L_0$, ..., and $\pm 102L_0$.

For measurement of critical current of the central section, the voltage probes were attached at $x = -L_0/2$ and $+L_0/2$. For measurement of critical current of the non-central sections, the voltage probes were attached in step of $-L_0$ from $-L_0/2$ in $-x$ direction and also in step of L_0 from $L_0/2$ in $+x$ direction.

The region between the voltage probes is called simply as region. The region containing the central section is called as the central region. Other regions are called as non-central regions. The voltage probe spacing L (= length of region in the longitudinal direction of the tape) was varied from L_0 to $3L_0$, $5L_0$, ..., and $41L_0$. For each of the voltage probe spacing $L = kL_0$ ($k = 1, 3, 5, \ldots$, and 41), the voltage-current curve and critical current of the central region consisting of k sections were obtained by attaching the voltage probes at $x = -kL_0/2$ and $kL_0/2$. The critical current of the other regions were obtained by attaching the voltage probes in step of $-kL_0$ from $x = -kL_0/2$ in $-x$ direction and also in step of kL_0 from $kL_0/2$ in $+x$ direction for $k = 1, 3, 5, \ldots$, and 41.

2.2 Calculation of voltage–current curve and critical current of non-central sections

For description of the voltage (V)–current (I) curves of cracked sections, we have been employing the model of Fang *et al.*[13] in a modified form,[4,5,7,9–12,22] with which the experimental results of critical current and n-value of stress-damaged filamentary- and coated-superconductors have been described. The modified form was used also in this work. Details are shown in our preceding works.[10–12] The outline is briefly described as follows.

In the transverse cross-section in which a partial crack (= the crack that exists in a part of transverse cross-section of the superconducting phase) exists, the cracked- and the ligament-parts constitute a parallel electric circuit. The ratio of cross-sectional area of cracked part to the total cross-sectional area of the superconducting layer is expressed by f. The ligament part with an area ratio $1 - f$ transports current I_{RE}. At the cracked part with an area ratio f, current I_s ($= I - I_{RE}$) shunts into stabilizer such as Ag and Cu. The electric resistance of the shunting circuit is noted as R_t. The voltage, developed at the ligament part that transports current I_{RE}, is noted as V_{RE}. The voltage $V_s = I_s R_t$, developed at the cracked part by shunting current I_s, is equal to V_{RE}, since the cracked- and ligament-parts constitute a parallel circuit. Noting the current transfer length as s ($\ll L_0$), the I_c and n-value of the sections in the non-cracked state as I_{c0} and n_0, respectively, and the critical electric field for determination of critical current as E_c (= 1 μV/cm in this work), we can express the V–I relation of the cracked section ($L_0 = 1.5$ cm) as,[4,5,9–12,22]

$$V = E_c L_0 (I/I_{c0})^{n_0} + V_{RE} \quad (1)$$

$$I = I_{RE} + I_s = I_{c0} L_{p,\,section} [V_{RE}/(E_c L_0)]^{1/n_0} + V_{RE}/R_t \quad (2)$$

The term $L_{p,\,section}$ in eq. (2) is given by $L_{p,\,section} = (1 - f)(L_0/s)^{1/n_0}$. This term is proportional to the ligament area ratio $1 - f$. It is, hereafter, called as a ligament parameter of section. The parameter $L_{p.section}$ was derived by the authors[4,5] by modifying the formulations of Fang *et al.*[13] In this work, as well as in our recent works,[10–12] it was used as a monitor of crack size (the smaller the ligament parameter, the larger is the crack size f.)

Wide distribution of ligament parameter $L_{p,\,section}$(= $(1 - f)(L_0/s)^{1/n_0}$) corresponds to wide distribution of f (crack size), since the standard deviation of $1 - f$ is the same as that of f. Thus the standard deviation of $L_{p,\,section}$, $\Delta L_{p,\,section}$, can be used as a monitor of the width of crack size distribution; the larger the $\Delta L_{p,\,section}$, the wider the crack size distribution. For formulation of distribution of $L_{p,\,section}$ of cracked sections with a length L_0, the normal distribution function was used, as in the preceding works.[10–12] Noting the average of $L_{p,\,section}$ as $L_{p,\,section,\,ave}$, the cumulative probability $F(L_{p,\,section})$ is expresses as

$$F(L_{p,\,section}) = \frac{1}{2}\left\{1 + \mathrm{erf}\left(\frac{L_{p,\,section} - L_{p,\,section,\,ave}}{\sqrt{2}\Delta L_{p,\,section}}\right)\right\} \quad (3)$$

In this work, $L_{p,\,section,\,ave} = 0.940$ and $\Delta L_{p,\,section} = 0.05$ were used to give the value of $L_{p,\,section}$ for each section except the central one by a Monte Carlo method: the $L_{p,\,section}$-value for each cracked section was obtained by generating a random value RND in the range of 0∼1, setting $F(L_{p,\,section}) = RND$ and substituting the values of $L_{p,\,section,\,ave} = 0.940$ and $\Delta L_{p,\,section} = 0.05$ in eq. (3).

The V–I curve of each cracked section except the central one was calculated by substituting the $L_{p,\,section}$-value stated

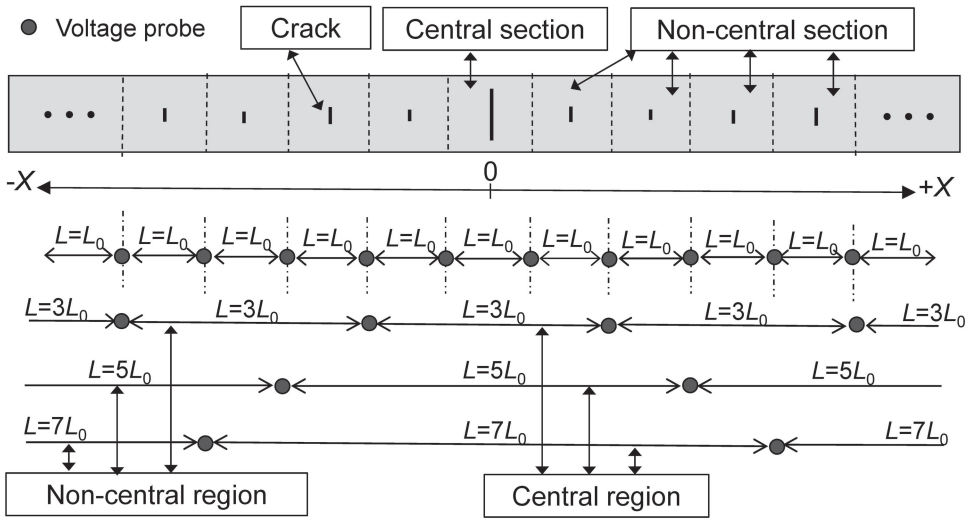

Fig. 2 Schematic representation of the model tape consisting of the sections with a length $L_0 = 1.5$ cm, together with the x coordinate and position of cracks. The section in the center of the model specimen, existing between $x = -L_0/2$ and $+L_0/2$, is called as the central section. Other sections are called as non-central sections. The voltage probe spacing L (= length of region between the voltage probes) were taken to be L_0, $3L_0$, $5L_0$, $7L_0$, …, $41L_0$ for measurement of current. The region containing the central section is called as the central region. Other regions are called as non-central regions.

above, and the values of $R_t = 2\,\mu\Omega$, $I_{c0} = 200$ A and $n_0 = 40$ into eqs. (1) and (2). Here, the values of I_{c0} and n_0 were taken from the experimental result[7] of a copper-stabilized DyBCO tape test-pieces, whose V–I curves were measured at 77 K in a self-magnetic field for the voltage probe spacing 1.5 cm. The R_t-value (= 2 μΩ) was taken from the average value obtained by analysis of the V–I curves of the test-pieces in which the superconducting DyBCO layer was cracked under various applied tensile stresses.

The critical current values of the sections, $I_{c,\,section}$, were obtained from the calculated V–I curves, by using the electric field criterion of $E = E_c = 1\,\mu V/cm$ (corresponding to $V = V_c = E_c L_0 = 1.5\,\mu V$).

2.3 Modeling of the crack size of the central sections

The values of critical current $I_{c,\,section}$ of the sections except the central one were obtained by the procedure stated in subsection 2.2. The obtained $I_{c,\,section}$–values of non-central sections, shown with the open circles, are plotted against position x in Fig. 3. The $I_{c,\,section}$–value varies with position, giving the local critical current-information.

After obtaining the variation of critical current of non-central sections along the longitudinal direction, we set the critical current (and hence the size of the crack monitored by the ligament parameter) of the central section for the five cases A, B, C, D and E, as follows.

The average of the critical current of the non-central sections was 189 A. The critical current of the central section, $I_{c,\,section,\,x=0}$, was taken as this average value in case A, corresponding to the ligament parameter $L_{p,\,section,\,x=0} = 0.940$. In case B, $I_{c,\,section,\,x=0}$ was taken to be 166 A, corresponding to $L_{p,\,section,\,x=0} = 0.826$. $I_{c,\,section,\,x=0} = 166$ A was chosen since it was equal to the lowest critical current value among the non-central sections. In cases C, D and E, the values of $I_{c,\,section,\,x=0}$ were set to be 152 A, 125 A and 102 A, respectively, which were lower than the lowest $I_{c,\,section}$ value (166 A) among the non-central sections. The corresponding values of $L_{p,\,section,\,x=0}$ were 0.757, 0.622 and 0.508 in cases C, D and E, respectively. They are smaller than 0.940 (case A) and 0.826 (case B), which shows directly that the ligament of the central section was set to be smaller and hence the crack of the central section was set to be larger than any of the non-central sections in cases C, D and E. In this way, in the present work, the central section corresponds to the largest crack-section in cases B, C, D and E. Only in case A, the central section does not correspond to the largest crack-section.

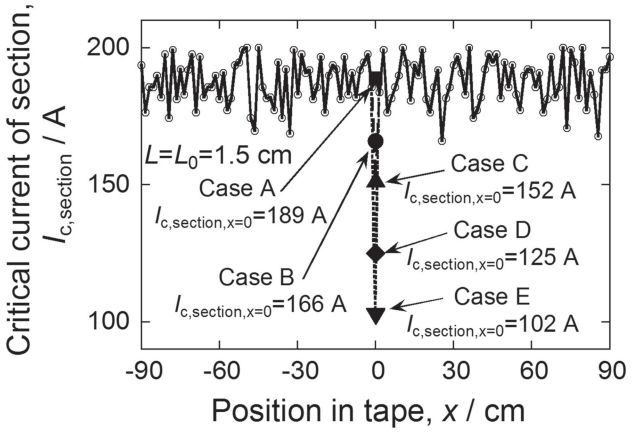

Fig. 3 Variation of critical current of sections, $I_{c,\,section}$, with position in cases A, B, C, D and E. The critical current values of non-central sections were given by the procedure stated in subsection 2.2. These values are common in cases A to E. The critical current values of the central section, $I_{c,\,section,\,x=0}$, in cases A to E were set to be 189 A, 166 A, 152 A, 125 A and 102 A, respectively.

2.4 Calculation of voltage (V)–current (I) curve of regions between the voltage probes

The V–I curve of each section is calculated by substituting the values of L_0, $L_{p,\,section}$, R_t, I_{co} and n_0 into eqs. (1) and (2). As the region consists of a series electric circuit of sections

(Fig. 2), the current of the region is the same as that of all sections, and the voltage of the region is the sum of the voltages of all sections. Noting the current of the region consisting of k-sections as $I_{\text{region},k}$, voltage of the region as $V_{\text{region},k}$, current of section i as $I_{\text{section},i}$, and voltage of section i as $V_{\text{section},i}$, the $V_{\text{region},k}$–$I_{\text{region},k}$ curve is calculated under the conditions of

$$I_{\text{region},k} = I_{\text{section},i} \quad (i = 1 \text{ to } k, k = 1 \text{ to } 41) \tag{4}$$

$$V_{\text{region},k} = \sum_{i=1}^{k} V_{\text{section},i} \quad (k = 1 \text{ to } 41) \tag{5}$$

Using the V–I curves of sections ($L_0 = 1.5$ cm) obtained by eqs. (1) and (2), we calculated the V–I curves of the regions by eqs. (4) and (5). Then we obtained the critical current values of the regions from the calculated V–I curves, with the electric field criterion of $E = E_c = 1\,\mu\text{V/cm}$ (corresponding to $V = V_c = E_c L\,\mu\text{V}$) for the voltage probe spacing $L = L_0$ (1.5 cm), $3L_0$ (4.5 cm), $5L_0$ (7.5 cm), ..., and $41L_0$ (61.5 cm).

3. Results and Discussion

3.1 Voltage (V)–current (I) curves of the region and the sections that constitute the region

Figure 4 shows the voltage (V)–current (I) curves of the 25.5 cm-central region between the voltage probes at the positions $x = -12.75$ cm and $+12.75$ cm and the sections that constitute the central region, for cases (a) A, (b) B, (c) C, (d) D and (e) E. In the cases A to E, the V–I curve of the central section is different from each other while the V–I curves of the non-central sections are common. The solid curves show the V–I curves of the central region. The line-dot curves and the dotted curves show the V–I curve of the section with the largest crack (= the section with the lowest critical current) and the V–I curves of the other sections, respectively. As stated in subsection 2.3, in case A (Fig. 4(a)), the critical current of the central section, $I_{\text{c, section, }x=0}$ was taken to be the same as the average value (189 A) and hence it was not identical to the critical current of the largest crack-section, $I_{\text{c, largest crack-section}}$ (175 A). In cases B to E, the largest crack exists in the central section and hence $I_{\text{c, section, }x=0}$ is the same as $I_{\text{c, largest crack-section}}$.

In case A, the difference in crack size among the sections is small. Hence the V_{section}–I curves exist in a narrow range of current. The size of the largest crack among the sections in the central region increases from case A to case E. Accordingly, the V_{region}–I curve of the central region shifts to lower current range, and the distance between the V_{section}–I curve of the largest crack-section and the V_{section}–I curves of the other sections increases with increasing size of the largest crack. As a result, the V_{region}–I curve is governed by the $V_{\text{largest crack-section}}$–$I$ curve up to higher voltage in case B, C, D and E. The dominant contribution of $V_{\text{largest crack-section}}$ to V_{region} is a feature of the V_{region}–I curve under co-existence of a large crack and multiple small cracks in the region.

Multiple cracks are contained in the region consisting of a series of sections (Fig. 2). The voltage developed in the largest crack-section contributes most to the voltage of the region in comparison with the voltages developed in other sections containing smaller cracks. In this subsection, by using the V–I curve of the largest crack-section in cases A to E (Fig. 4), we derive the upper and lower bounds of V_{region}–I curve of the central region, $V_{\text{region, upper}}$–I and $V_{\text{region, lower}}$–I curves, respectively, and then the upper and lower bounds of $I_{\text{c, region}}$ (critical current of region) of the central region, $I_{\text{c, region, upper}}$ and $I_{\text{c, region, lower}}$, respectively. Then we compare them with the V_{region}–I curves in Fig. 4 and also discuss the factor that contribute to raise the critical current values of the

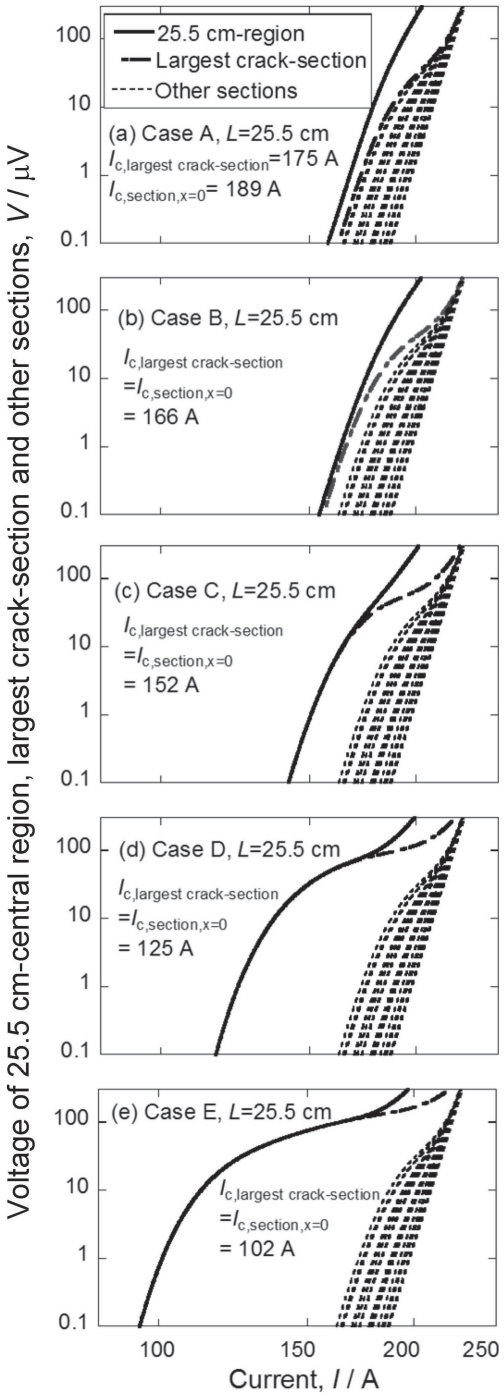

Fig. 4 Voltage (V)–current (I) curves of the 25.5 cm-central region and the sections that constitute the central region, in cases (a) A, (b) B, (c) C, (d) D and (e) E. The V–I curve of the region is presented with solid curve. The V–I curve of the section with the largest crack (= the section with the lowest critical current) is shown with line-dot curve and that of the other sections with dotted curves.

regions with voltage probe spacing L (= length of the region) under co-existence of a large crack and multiple small cracks in cases B to E.

We take up two extreme situations to derive the upper and lower bounds of critical current of region.[12] In one extreme situation (1), the crack size in all sections is the same as that of the largest crack. In this situation (1), the $V_{section}$–I curve is the same in all sections, and the voltage of the region between the voltage probes, given by the sum of the voltage values of the sections, is the upper bound of the voltage, $V_{region, upper}$. Accordingly, the voltage developed in the region reaches the critical voltage V_c for determination of critical current at low I. Thus the situation (1) gives the lower bound, $I_{c, region, lower}$, for critical current. In another extreme situation (2), the crack size of one section is far larger than that of the other sections, as in cases C, D and E. In this situation (2), the voltage developed in the region is almost the same as that developed just in the largest crack-section. Namely, the voltages developed at the other sections are very low and do not contribute to the voltage of the region. Thus, the situation (2) gives the lower bound for the voltage of the region, $V_{region, lower}$. As the voltage of the region reaches V_c at high I, the situation (2) gives the upper bound of critical current of the region, $I_{c, region, upper}$. In this way, the situation (1) gives $V_{region, upper}$–I curve and $I_{c, region, lower}$, and the situation (2) gives $V_{region, lower}$–I curve and $I_{c, region, upper}$.

The $V_{region, upper}$–I and $V_{region, lower}$–I curves were calculated by substituting the aforementioned values of $L_{p, section}$ and R_t for the largest crack-section into eqs. (1), (2), (4) and (5). Figure 5 shows the V_{region}–I curves taken from Fig. 4 and the calculated $V_{region, upper}$–I and $V_{region, lower}$–I curves for comparison. The V_{region}–I curve in each case (A to E) is in between the $V_{region, upper}$–I and $V_{region, lower}$–I curves. It is important that, in case A, the V_{region}–I curve exists in the middle between the $V_{region, upper}$–I and $V_{region, lower}$–I curves (Fig. 5(a)), but, then, with increasing size of the largest crack as in cases B to D, the V_{region}–I curve shifts to $V_{region, lower}$–I curve (Fig. 5(b–e)).

Due to the shift of the V_{region}–I curve mentioned above, the $I_{c, region}$ value shifts from the middle between the $I_{c, region, lower}$ and $I_{c, region, upper}$ to the $I_{c, region, upper}$ with increasing size of the largest crack. Figure 6 shows the critical current $I_{c, region}$ and its lower ($I_{c, region, lower}$) and upper ($I_{c, region, upper}$) bounds in cases A to E of 25.5 cm-region, plotted against the critical current of the largest crack-section, $I_{c, largest\ crack\text{-}section}$, where the $I_{c, region}$, $I_{c, region, lower}$ and $I_{c, region, upper}$ values were estimated from the V_{region}–I, $V_{region, upper}$–I and $V_{region, lower}$–I curves in Fig. 5. The result in Fig. 6 shows clearly that the $I_{c, region}$ shifts to $I_{c, region, upper}$ with decreasing $I_{c, largest\ crack\text{-}section}$ (with increasing size of the largest crack).

Figure 7 shows the V_{region} (voltage developed in region)–I (current), $V_{largest\ crack\text{-}section}$ (voltage developed at the largest crack-section)–I (current), and $V_{largest\ crack\text{-}section}$–$I_{RE, largest\ crack\text{-}section}$ (current transported by the ligament part of the REBCO layer in the largest crack-section) curves, calculated for the voltage probe spacing $L = 25.5$ cm in case D. a and b refer to the increment of REBCO transported current and shunting current, respectively, which are induced by changing the voltage probe spacing from 1.5 cm to 25.5 cm. As the shunting current at $V = V_c = 1.5\ \mu V$ (shown

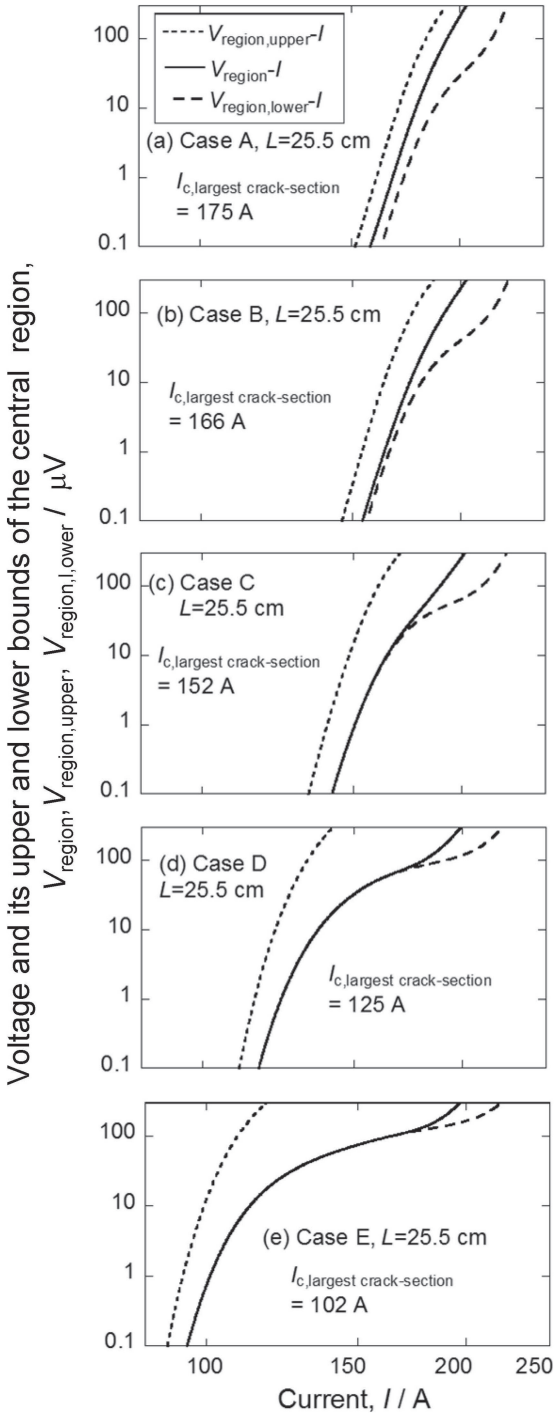

Fig. 5 V_{region}–I curves taken from Fig. 4 and the calculated $V_{region, upper}$–I and $V_{region, lower}$–I curves for comparison.

by the difference in current between the $V_{largest\ crack\text{-}section}$–$I$ and $V_{largest\ crack\text{-}section} - I_{RE, largest\ crack\text{-}section}$ curves at $V = V_c = 1.5\ \mu V$), is low, the difference in critical current between the 25.5 cm-region and 1.5 cm-section with the largest crack is given by $a + b$. In this example (Fig. 7), a and b were 9 A and 12 A, respectively. In this way, the increase in critical current of the region with increasing voltage probe spacing was accounted for by the enhanced REBCO transported current and shunting current in accordance with the increase in V_c under the 1 μV/cm criterion.

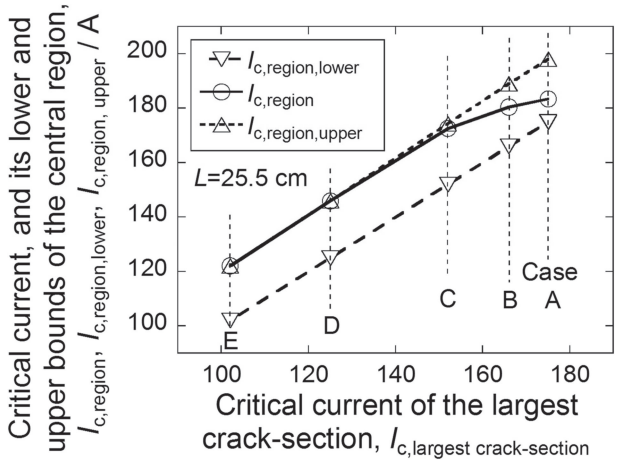

Fig. 6 Critical current $I_{c,\,region}$ of 25.5 cm-region and its lower ($I_{c,\,region,\,lower}$) and upper ($I_{c,\,region,\,upper}$) bounds in cases A to E, plotted against the critical current of the largest crack-section, $I_{c,\,largest\ crack\text{-}section}$. The result shows that the $I_{c,\,region}$ shifts to $I_{c,\,region,\,upper}$ with decreasing $I_{c,\,largest\ crack\text{-}section}$ (with increasing size of the largest crack).

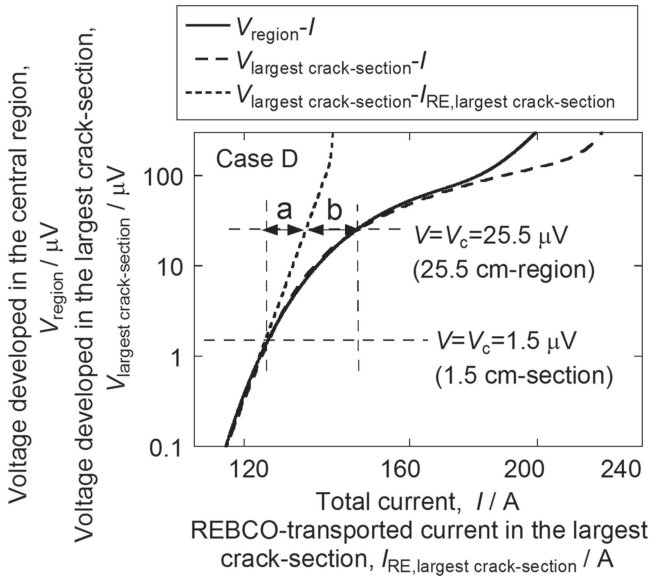

Fig. 7 Calculated V_{region} (voltage developed in 25.5 cm-region)–I (current), $V_{largest,\,crack\text{-}section}$ (voltage developed at the largest crack-section)–I (current), and $V_{largest\ crack\text{-}section} - I_{RE,\,largest\ crack\text{-}section}$ (current transported by the ligament part of the REBCO layer in the largest crack-section) curves in case D. $a + b$ corresponds to the increment of critical current with increase in the voltage probe spacing from 1.5 cm to 25.5 cm, where a and b refer to the increment of REBCO transported current and shunting current, respectively.

3.2 Influence of voltage probe spacing (L) on the voltage (V)–current (I) curve, electric field (E)–current (I) curve of the central region

Figure 8(a), (b) and (c) show the voltage (V)–current (I) curves and Fig. 8(a′), (b′) and (c′) show the electric field (E)–current (I) curves of the central regions, obtained by simulation for the voltage probe spacing $L = 1.5$ to 61.5 cm in cases (a, a′) A, (b, b′) C and (c, c′) E. In calculation, the V–I curves of the non-central sections were taken to be common and only the size of the crack in the central section was changed in cases A to E.

In case A, the critical current of the central section was taken to be equal to the average of I_c values of non-central sections, 189 A. In this case, as the difference in crack size between the central section and non-central sections is small, the voltages developed at all sections contribute to the synthesis of the voltage of the region. Thus the voltage of the V–I curve of the region consisting of the sections for a given current increases with increasing L. In this case, the V–I

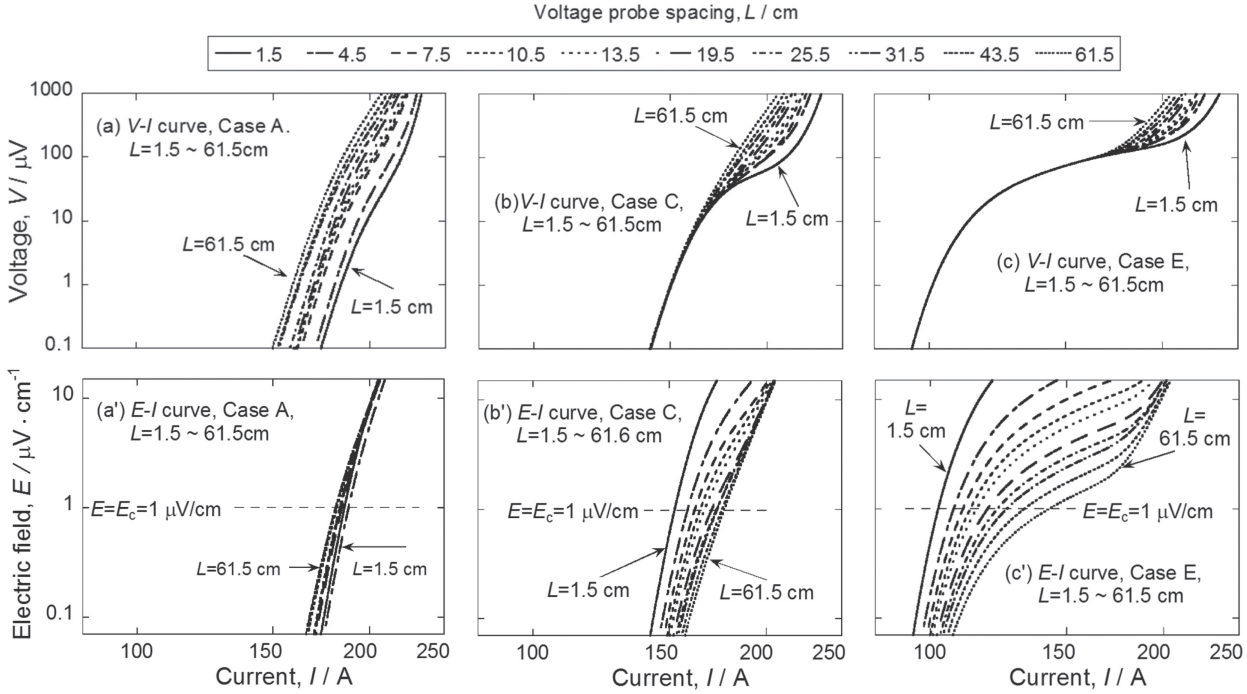

Fig. 8 (a), (b), (c) Voltage (V)–current (I) curves and (a′), (b′), (c′) electric field (E)–current (I) curves of the central regions for $L = 1.5$ to 61.5 cm in cases (a), (a′) A, (b), (b′) C and (c), (c′) E.

curves of the regions for different L are different from each other. The feature of case A is found also in the non-central regions that have no accidental large crack.

In case A, the size of the largest crack in the region is dependent on the voltage probe spacing L; it increases with increasing L. Reflecting this tendency, the critical current decreases with increasing L. On the other hand, in cases B∼E, the largest crack existing in the central section is contained in the central region for any voltage probe spacing. Accordingly, in contrast to case A, the size of the largest crack in the central region does not vary with voltage probe spacing in cases B to E. Reflecting this feature, when the largest crack is far larger than the other cracks, the voltage is developed only at the largest crack-section and therefore the V–I curve of the region is determined by the V–I curve of the largest crack-section up to some voltage level; the voltage-current curve of the region, V_{region}–I, is the same as that of the largest crack-section, $V_{\mathrm{largest\,crack\text{-}section}}$–$I$, up to $V \approx 10\,\mu\mathrm{V}$ as in case C (Fig. 8(b)). When the largest crack is far larger than other cracks as in case E (Fig. 8(c)), the V_{region}–I curve is the same as that of the $V_{\mathrm{largest\,crack\text{-}section}}$–$I$ curve up to higher voltage level ($V \approx 100\,\mu\mathrm{V}$). At further higher voltage level ($V > 100\,\mu\mathrm{V}$), not only the voltage developed at the largest crack-section but also the voltages developed at other sections contribute to the voltage of the central region. The larger the L, the larger becomes the number of cracks that contribute to raise the voltage of the region. Thus, beyond the voltage level below which only the largest crack-section contributes to the voltage of the region, the increase in voltage of the region is enhanced with increase in L, as shown in Fig. 8(b) and (c).

The V–I curves in Fig. 8(a), (b), (c) were converted to E–I curves, as shown in Fig. 8(a′), (b′), (c′). In contrast to the V–I curves, the E–I curve at each L is clearly distinguished, from which critical current (I_c) was obtained with the $E_c = 1\,\mu\mathrm{V/cm}$ criterion.

3.3 Change in critical current of the central and non-central regions with increasing voltage probe spacing

The representative results of the critical current values of the central and non-central regions are plotted against position along the longitudinal direction of the tape, as shown in Fig. 9. (a1)∼(a5), (b1)∼(b5), (c1)∼(c5), (d1)∼(d5) and (e1)∼(e5) refer to the cases A, B, C, D and E, respectively. (a1)∼(e1), (a2)∼(e2), (a3)∼(e3), (a4)∼(e4) and (a5)∼(e5) refer to the voltage probe spacing $L = 1.5$, 4.5, 13.5, 37.5 and 61.5 cm, respectively. The critical current value of the central region is noted in each figure. Figure 10 shows the change in critical current of the central region with increasing voltage probe spacing in cases A to E. From the results in Figs. 9 and 10, the following influences of the voltage probe spacing on the variation of critical current value with position are read.

(a) In case A, the critical current 189 A of the central section was taken to be equal to the average critical current of the non-central sections. Therefore, half of the non-central sections have larger but half of them have smaller cracks than

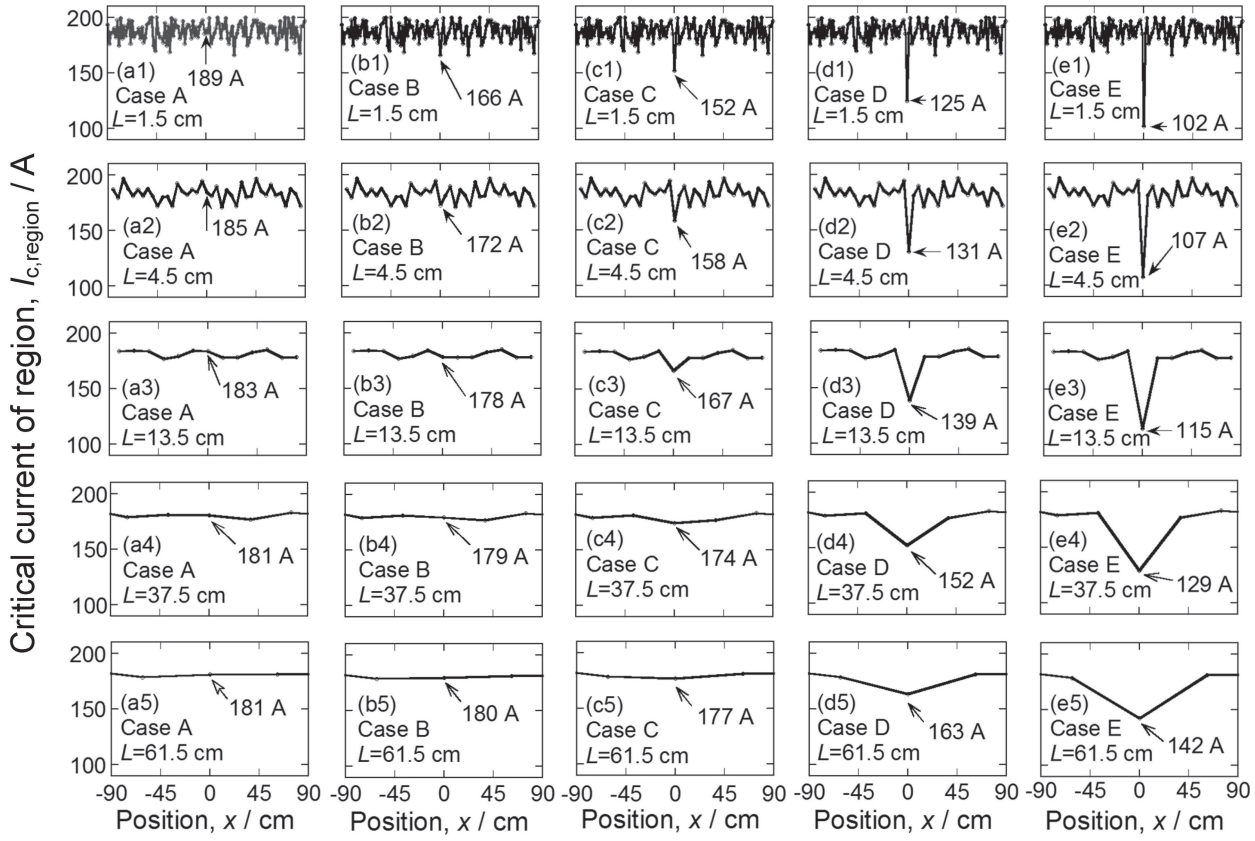

Fig. 9 Influence of the voltage probe spacing on the variation of critical current value with position. (a1)∼(a5), (b1)∼(b5), (c1)∼(c5), (d1)∼(d5) and (e1)∼(e5) refer to the cases A, B, C, D and E, respectively. (a1)∼(e1), (a2)∼(e2), (a3)∼(e3), (a4)∼(e4) and (a5)∼(e5) refer to the voltage probe spacing $L = 1.5$, 4.5, 13.5, 37.5 and 61.5 cm, respectively.

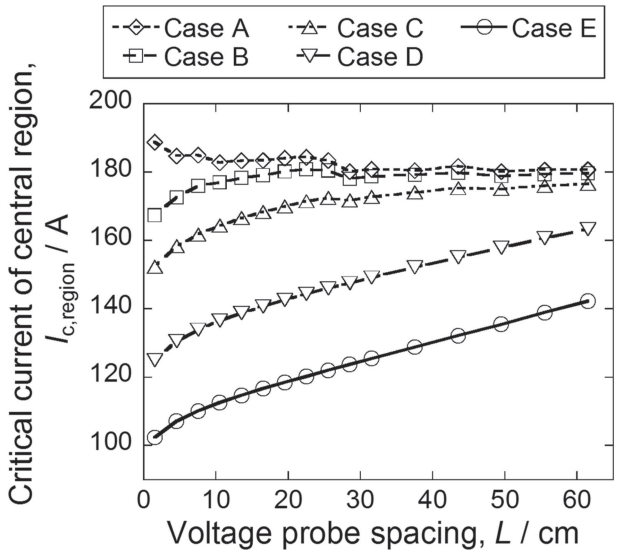

Fig. 10 Change in critical current $I_{c,region}$ of the central region with increasing voltage probe spacing in cases A to E.

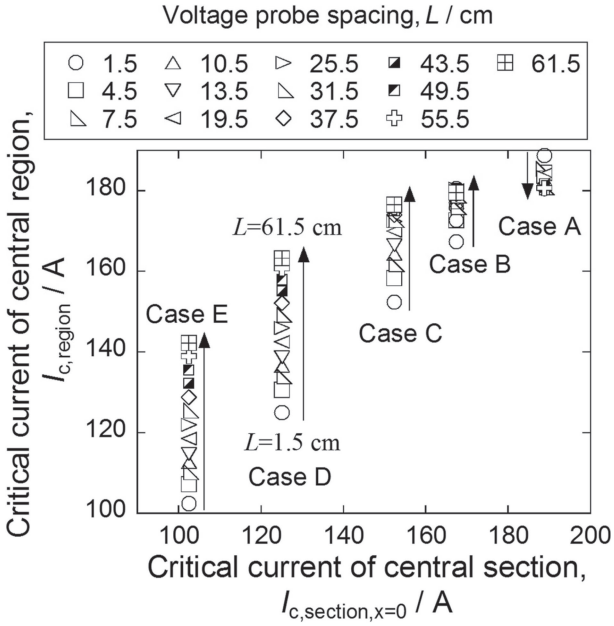

Fig. 11 Change in critical current $I_{c,region}$ of the central region that contains central section whose critical current $I_{c,section,x=0}$ was 102 A (case E), 125 A (case D), 152 A (case C), 166 A (case B) and 189 A (case A), respectively.

the central section. In the process of the increase in voltage probe spacing from $L + \Delta L$, if the neighboring sections with larger cracks are added to the central region, critical current for $L + \Delta L$ becomes lower than that for L. On the other hand, if the neighboring sections with smaller cracks are added to the central region, the critical current for larger $L + \Delta L$ becomes higher than that for L due to the increase in the critical voltage V_c ($= E_c L$), which enhances the REBCO ligament-transported current I_{RE} and the shunting current I_s (Fig. 7). In this way, in the process of increase in L, if the sections newly added to the central region have smaller and larger cracks than the largest crack existing already, the critical current of the central region goes up and goes down, respectively. Such a zig-zag variation of critical current with L is realized in case A in Fig. 10.

(b) While case A shows zig-zag variation of critical current, the critical current tends to decrease with increasing L since the number of cracks increases and hence the size of the largest crack among all cracks in the region increases. This situation is the same as that in the non-central regions. Accordingly, the critical current of the central region as well as the non-central regions decreases with increasing L (Fig. 9((a1)~(a5)) and Fig. 10).

(c) In contrast to case A where critical current of the central region decreases with increasing L, critical current value increases with increasing L in cases B to E, due to the increase in V_c ($= E_c L$), which enhances the REBCO ligament-transported current and shunting current (Fig. 7).

(d) The critical current of the central region in cases B and C, where the difference in size between the largest crack and other cracks is relatively small in comparison with that in cases D and E, increases with increasing L and reaches almost the level of non-central regions. This result is in good accordance with the experimentally observed phenomenon in the sample with one large defect.[23)]

(e) When the difference in size between the largest crack and other cracks is large, as in cases D and E, the critical current also increases with increasing L, but not reach the critical current level within the present range of $L =$ 1.5~61.5 cm.

(f) The extent of the variation of critical current with position of the non-central regions also decreased with increasing L (Fig. 9), which also reproduces well the experimentally observed feature that the local critical current information is diluted for large L.[23)]

Figure 11 shows the change in critical current, $I_{c,region}$, of the central region that contains central section whose critical current $I_{c,section,x=0}$ was 102 A (case E), 125 A (case D), 152 A (case C), 166 A (case B) and 189 A (case A), respectively. In case A, where the central section has a critical current-value equal to average critical current of sections, the critical current of the region decreases with increasing L due to the increase of size of the largest crack with increasing L. On the other hand, when the central section has the largest crack, namely, has the lowest critical current among the sections, the $I_{c,region}$ increases with increasing L. It is noted that the extent of the increase in critical current is higher for lower $I_{c,section,x=0}$ (for larger crack) (Fig. 11), since only the voltage developed at the largest crack-section contributes to the synthesis of the voltage of the region, as shown by the current range in Fig. 8(b) and (c) where the V–I curve of the region is equal to that of the largest crack-section. This situation acts to minimize the V in the relation between V and I, and gives the high critical current value for the region.

4. Conclusions

A simulation study was conducted to describe the dependence of critical current value obtained by the 1 μV/cm criterion on the voltage probe spacing under the co-existence of a large accidental crack and multiple small cracks. The main results are summarized as the followings.

(1) The experimentally observed feature, "when a large accidental crack is included in the region between the voltage probes, the critical current value increases with increasing voltage probe spacing", was reproduced by the present simulation method.
(2) It was confirmed that the local critical current-information is diluted when the voltage probe spacing is large under occurrence of heterogeneous cracking of superconducting layer.
(3) The voltage-current curve of the section containing a large crack contributes largely to the synthesis of the voltage-current curve of the region between the voltage probes and, hence, contributes to the determination of critical current value of the region. This feature becomes more dominant when the difference in size between the large crack and the small cracks is larger.
(4) The critical current value of the region containing a large crack and multiple small cracks increases with increasing voltage probe spacing up to the critical current level determined by the small cracks.
(5) Using the voltage-current curve of the section with a largest crack, the upper and lower bounds of the critical current of the region consisting of a section with a large crack and multiple sections with small cracks could be estimated. It was shown that, when the difference in size between the large crack and small cracks is large, the critical current of the region is given by the upper bound for a given size of the largest crack.

REFERENCES

1) N. Cheggour, J.W. Ekin and C.C. Clickner: Appl. Phys. Lett. **83** (2003) 4223–4225.
2) D. Uglietti, B. Seeber, V. Abächerli, W.L. Carter and R. Flükiger: Supercond. Sci. Technol. **19** (2006) 869–872.
3) D.C. van der Laan, J.W. Ekin, F.F. Douglas, C.C. Clickner, T.C. Stauffer and L.F. Goodrich: Supercond. Sci. Technol. **23** (2010) 072001.
4) S. Ochiai, T. Arai, A. Toda, H. Okuda, M. Sugano, K. Osamura and W. Prusseit: J. Appl. Phys. **108** (2010) 063905.
5) S. Ochiai, H. Okuda, T. Arai, S. Nagano, M. Sugano and W. Prusseit: Cryogenics **51** (2011) 584–590.
6) H.S. Shin, J. Marlon, H. Dedicatoria, H.S. Kim, N.-J. Lee, H.S. Ha and S.S. Oh: IEEE Trans. Appl. Supercond. **21** (2011) 2997–3000.
7) S. Ochiai, H. Okuda, T. Arai, M. Sugano, K. Osamura and W. Prusseit: J. Japan Inst. Copper "Copper and Copper Alloys" **53** (2013) 225–230.
8) H. Oguro, T. Suwa, T. Suzuki, S. Awaji, K. Watanabe, M. Sugano, S. Machiya, M. Sato, T. Koganezawa, T. Machi, M. Yoshizumi and T. Izumi: IEEE Trans. Appl. Supercond. **23** (2013) 8400304.
9) S. Ochiai, H. Okuda, M. Sugano, S.-S. Oh and H.-S. Ha: Mater. Trans. **55** (2014) 549–555.
10) S. Ochiai, H. Okuda and N. Fujii: Mater. Trans. **58** (2017) 679–687.
11) S. Ochiai, H. Okuda and N. Fujii: Mater. Trans. **58** (2017) 1469–1478.
12) S. Ochiai, H. Okuda and N. Fujii: Mater. Trans. **59** (2018) 1628–1636.
13) Y. Fang, S. Danyluk and M.T. Lanagan: Cryogenics **36** (1996) 957–962.
14) T. Kiss, H. van Eck, B. ten Haken and H.H.J. ten Kate: IEEE Trans. Appl. Supercond. **11** (2001) 3888–3891.
15) H. Kitaguchi, H. Kumakura and K. Togano: Physica C **363** (2001) 198–201.
16) H. Kitaguchi, A. Matsumoto, H. Hatakeyama and H. Kumakura: Physica C **401** (2004) 246–250.
17) N. Banno, D. Uglietti, B. Seeber, T. Takeuchi and R. Flükiger: Supercond. Sci. Technol. **18** (2005) 284–288.
18) S. Ochiai, J.K. Shin, S. Iwamoto, H. Okuda, S.S. Oh, D.W. Ha and M. Sato: J. Appl. Phys. **103** (2008) 123911.
19) S. Ochiai, M. Fujimoto, H. Okuda, S.S. Oh and D.W. Ha: J. Appl. Phys. **105** (2009) 063912.
20) Y. Miyoshi, E.P.A. Van Lanen, M.M. Dhallé and N. Nijhuits: Supercond. Sci. Technol. **22** (2009) 085009.
21) S. Ochiai, H. Okuda, M. Sugano, M. Hojo and K. Osamura: J. Appl. Phys. **107** (2010) 083904.
22) S. Ochiai, H. Okuda, M. Sugano, K. Osamura, A. Otto and A.P. Malozemoff: Mater. Trans. **57** (2016) 709–715.
23) J.J. Gannon, Jr., A.P. Malozemoff, R.C. Diehl, P. Antaya and A. Mori: IEEE Trans. Appl. Supercond. **23** (2013) 8002005.
24) T. Nakamura, Y. Takamura, N. Amemiya, K. Nakao and T. Izumi: Cryogenics **63** (2014) 17–24.